applied mechanics

Article

Theoretical Assessment of Cracking in Orthotropic Material under Symmetrical Heat Flow/Mechanical Loading

Bing Wu [1], Daren Peng [2,*] and Rhys Jones [2]

[1] Co-Technology Innovation Center for Testing and Evaluation in Civil Engineering of Hebei Province, Baoding 071002, China; bingwu@hub.edu.au
[2] Centre of Expertise Structural Mechanics, Department of Mechanical and Aerospace Engineering, Monash University, Clayton, VIC 3800, Australia; rhys.jones@monash.edu
* Correspondence: daren.peng@monash.edu

Abstract: This paper studies a cracked orthotropic solid under symmetric heat flow, and symmetric mechanical loading is studied. A modified partially impermeable crack model is employed to simulate thermal load transfer. With the application of the Fourier transform technique and superposition theory, the related physical quantities and fracture parameters are obtained in explicit forms. The advantage of this paper is that the obtained solutions are explicitly closed. As a result, the calculation of the stress intensity factors of various cracks with different lengths becomes very convenient and fast. Some simple examples are used to demonstrate the method provided in this paper. The analysis results show the dimensionless thermal resistance (ϖ_c) between the upper and lower crack regions and the proposed coefficient (ε) greatly influence the related physical quantities and fracture parameters. In addition, the numerical analysis results also revealed that the calculated results of fracture parameters at the crack tip will not be physically meaningful unless certain conditions are met.

Keywords: modified partially impermeable crack; Fourier transform technique; physical quantity; thermal conductivity; the proposed coefficient

Citation: Wu, B.; Peng, D.; Jones, R. Theoretical Assessment of Cracking in Orthotropic Material under Symmetrical Heat Flow/Mechanical Loading. *Appl. Mech.* **2022**, *3*, 590–607. https://doi.org/10.3390/applmech3020035

Received: 31 March 2022
Accepted: 10 May 2022
Published: 13 May 2022

1. Introduction

Piezoelectric ceramics, multi-component composite materials, etc., are common materials in modern industry. However, defects or cracks inevitably exist in these materials due to factors in the production process, working environment, and material compositions. These cracks will reduce the load-bearing capacity of structures and even cause accidents/disasters. Therefore, due to the safety issue, it is necessary to use the theory of thermal elasticity to perform fracture analysis for cracked materials.

There have been many investigations and explorations on the fracture behavior of infinite bodies containing single or multiple cracks [1–4]. The singularity analysis of the thermal stress at the crack tips for a cracked solid under temperature difference or heat flux has been investigated [5,6]. Fracture parameters (i.e., mode-II stress intensity factors) of a single crack subject to thermal loading were obtained explicitly by Tsai [7]. By using a least-squares method, the expression of some fracture parameters with mix-mode was given by Ju and Rowlands [8]. The thermo-elasticity problem for a cracked solid under constant loading was taken into consideration by Chen and Zhang [9]. The stress analysis for cracked plates has been considered by Noda [10]. Fracture parameters in a semi-infinite medium have been studied by Rizk [11]. The mixed-mode fracture problem of functionally graded solids subject to mechanical loading was discussed by Kim and Paulino [12]. Furthermore, the thermoelectricity of orthotropic functionally graded solids has attracted extensive attention in the past decade. For example, the thermo-elastic problem of a cracked solid subject to plane temperature-step waves was investigated by Brock [13]. The fracture problem of cracked functionally graded solids subject to tensile by using the equivalent domain integral is formulated by Dag [14]. The closed forms of relevant fracture parameters for two collinear cracks subject to linear thermal flux have been obtained by Wu et al. [15]. Fracture analysis of cracked solids subjected to thermal loads has been studied extensively [16–20].

To solve more practical problems, this paper intends to expand the previous approach to solve the fracture problem of a cracked orthotropic material subjected to more complex loading. First, the modified partially impermeable crack model is used to study the thermoelastic problem of cracked material subject to symmetric thermal flux and mechanical. Second, Fourier transform is utilized to reduce the mixed boundary value problem to a set of dual integral equations. Solving these integral equations, the explicit forms of thermoelastic fields are obtained. Numerical results show great effects from the dimensionless thermal resistance (ϖ_c) between the upper and lower crack regions and the proposed coefficient (ε) on related physical quantities and fracture parameters.

In addition, it should be stressed that the fatigue crack growth prediction of a cracked component/structure is exceptionally difficult and computationally intensive, as calculations need to be made at each stage of the life of a component/structure. This is done to compute the stress intensity factors (K) for each crack configuration to calculate the amount of crack growth, update the crack geometry, and then re-compute the stress intensity factors for this new geometry. As the stress intensity factors obtained in this paper are theoretical solutions in explicit forms, it provides a quick, effective, and ideal analysis tool for the fatigue life/crack growth prediction of a cracked orthotropic material or structure under the combined action of mechanical and thermal loading.

2. Problem Statement

Let us consider the fracture problem of a single crack under thermal and mechanical loading, as shown in Figure 1. It is assumed that a single crack is situated on the part (i.e., $-a < x < a$). In this study, the heat flux $E(x)$ is only applied to one surface (such as the bottom surface) of the crack.

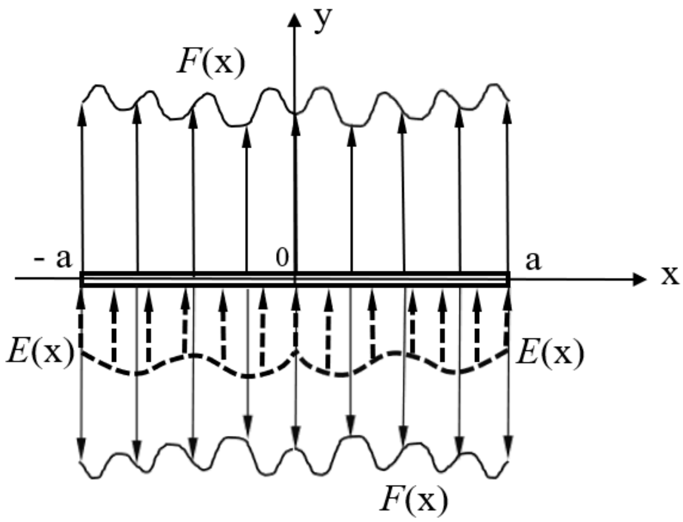

Figure 1. A single crack under symmetrical heat flow $E(x)$ and symmetrical mechanical loading $F(x)$.

For two-dimensional plane stress problems, the stresses for an orthotropic material [21] can be expressed as follow:

$$\sigma_{xx} = c_{11}\frac{\partial u}{\partial x} + c_{12}\frac{\partial v}{\partial y} - \beta_1 T \quad (1)$$

$$\sigma_{yy} = c_{12}\frac{\partial u}{\partial x} + c_{22}\frac{\partial v}{\partial y} - \beta_2 T \quad (2)$$

$$\sigma_{xy} = c_{66}[\frac{\partial u}{\partial y} + \frac{\partial v}{\partial x}] \tag{3}$$

where

$$c_{11} = \frac{E_{xx}}{1 - v_{xy}v_{yx}},\ c_{22} = \frac{E_{yy}}{1 - v_{xy}v_{yx}} \tag{4}$$

$$c_{12} = \frac{E_{xx}v_{yx}}{1 - v_{xy}v_{yx}} \tag{5}$$

$$\begin{bmatrix} \beta_1 \\ \beta_2 \end{bmatrix} = \begin{bmatrix} c_{11} & c_{12} \\ c_{12} & c_{22} \end{bmatrix} \begin{bmatrix} \alpha_{xx} \\ \alpha_{yy} \end{bmatrix} \tag{6}$$

where, $\sigma_{xy},\ \sigma_{yy}$, and σ_{xy} denote components of stress; u and v stand for components of the elastic displacements; E_{xx} and E_{yy} are the Young's moduli; $c_{66} = G_{xy}$ is the shear modulus; v_{xx} and v_{yy} are Poisson's ratios; T represents the temperature; α_{xx} and α_{yy} are the coefficient of thermal expansion. Substituting all stress expressions (1)–(3) into the following differential equations of equilibrium

$$\frac{\partial \sigma_{xx}}{\partial x} + \frac{\partial \sigma_{xy}}{\partial y} = 0,\ \frac{\partial \sigma_{xy}}{\partial x} + \frac{\partial \sigma_{yy}}{\partial y} = 0 \tag{7}$$

We obtain

$$c_{11}\frac{\partial^2 u}{\partial x^2} + c_{66}\frac{\partial^2 u}{\partial y^2} + (c_{12} + c_{66})\frac{\partial^2 v}{\partial x \partial y} = \beta_1 \frac{\partial T}{\partial x} \tag{8}$$

$$c_{66}\frac{\partial^2 v}{\partial x^2} + c_{22}\frac{\partial^2 v}{\partial y^2} + (c_{12} + c_{66})\frac{\partial^2 u}{\partial x \partial y} = \beta_2 \frac{\partial T}{\partial y} \tag{9}$$

In order to simulate the relationship between heat flux and temperature difference in cracked materials, a model called the 'modified partially impermeable crack model' is usually used, see Equation (10) [22–24]:

$$Q_c = -R_c \Delta T \tag{10}$$

where, Q_c, R_c, and ΔT stands for the heat flux per thickness of the crack surface, the thermal conductivity inside the cracks, and the difference of temperature between the crack faces, respectively. The value of $R_c \to 0$ or $R_c \to \infty$ denotes the perfectly thermally impermeable or permeable state of the crack surface. However, there may be impurities or thermal barriers in the cracks. To expand the function of Equation (10) to an improved new model called a modified partially impermeable crack model can be proposed as follows:

$$Q_c = -R_c \Delta T + \varepsilon Q_0 \tag{11}$$

where Q_0 and ε represent initial heat flux and a constant, which is considered to be arbitrary. $\varepsilon = 0$ in Equation (11) degenerates to the crack–face boundary condition of Equation (10).

Furthermore, the constant εQ_0 in Equation (11) is introduced for two main reasons. The first is simple: it is very difficult to for R_c which is usually regarded as a fixed constant to precisely address a crack full of thermal resistance through the crack area. Therefore, the constant εQ_0, which is marked as a self-adjusting factor, is used to model the actual situation. The second reason is that whether the coefficient ε is positive or not depends on the temperature field.

Utilizing the Fourier heat conduction, one obtains:

$$Q_x = -\lambda_x \frac{\partial T}{\partial x},\ Q_y = -\lambda_y \frac{\partial T}{\partial y} \tag{12}$$

where Q_x and Q_y are the components of the heat flux. λ_x and λ_y denote the heat conduction coefficient. Furthermore, based on the equilibrium equation, one obtains

$$\frac{\partial Q_x}{\partial x} + \frac{\partial Q_y}{\partial y} = 0 \tag{13}$$

With the aid of the thermal equilibrium equation, one has

$$\lambda^2 \frac{\partial^2 T}{\partial x^2} + \frac{\partial^2 T}{\partial y^2} = 0 \tag{14}$$

wherein

$$\lambda = \sqrt{\frac{\lambda_x}{\lambda_y}} \tag{15}$$

Making use of the boundary conditions causes

$$Q_y^I(x,0) - Q_y^{II}(x,0) = E(x) \ -a < x < a \tag{16}$$

$$\sigma_{yy}^{II}(x,0) = \sigma_{yy}^I(x,0) = F(x) \ -a < x < a \tag{17}$$

The superscript I or II denotes the part (i.e., $y > 0$ or $y < 0$). It is convenient to express symmetrical $E(x)$ by using their Taylor expansion.

$$E(x) = -\sum_{i=0}^{M} \frac{Q_{0i}}{2a^{i+1}} |x|^i, \quad -a < x < a \tag{18}$$

Similarly, the following symmetrical $F(x)$ are given explicitly.

$$F(x) = \sum_{j=0}^{k} \frac{\sigma_j}{a^j} |x|^j \quad -a < x < a \tag{19}$$

where Q_{0i} and σ_j denote the prescribed constant. The thermal flux and mechanical loading are symmetric on the x-axis, and the solution to this problem will be obtained explicitly.

3. The Solution to Symmetric Heat Flow and Mechanical Loading

Subject to symmetric thermal flux and mechanical loading, the closed form of the solution to the problem will be given in this section. The crack–face boundary conditions are written as

$$Q_y^I(x,0) - Q_y^{II}(x,0) = -\sum_{i=0}^{M} \frac{Q_{0i}}{2a^{i+1}} |x|^i \quad -a < x < a \tag{20}$$

$$\sigma_{yy}^{II}(x,0) = \sigma_{yy}^I(x,0) = \sum_{j=0}^{k} \frac{\sigma_j}{a^j} |x|^j \quad -a < x < a \tag{21}$$

Based on the symmetry of the thermomechanical loading, the half part (i.e., $x > 0$ and $-\infty < y < +\infty$) of the thermo-elastic field under thermomechanical loading $-\sum_{i=0}^{M} Q_{0i}|x|^i/2a^{i+1}$ and $\sum_{j=0}^{k} \sigma_j |x|^j/a^j$ is taken into account. The boundary conditions are expressed based on the modified partially impermeable crack model.

$$\sigma_{xy}^I(x,0) = \sigma_{xy}^{II}(x,0) = 0 \ -a < x < a \tag{22}$$

$$Q_y^I(x,0) - Q_y^{II}(x,0) = -\sum_{i=0}^{M} \frac{Q_{0i} - Q_{ci}}{2a^{i+1}} |x|^i \quad -a < x < a \tag{23}$$

$$\sigma_{yy}^{II}(x,0) = \sigma_{yy}^I(x,0) = \sum_{j=0}^{k} \frac{\sigma_j}{a^j} |x|^j \ -a < x < a \tag{24}$$

From Equations (23) and (24), the thermal flux and mechanical loading are made up of multiple sections. Firstly, the solutions subject to thermal flux $-Q_{0i}|x|^i/2a^{i+1}$ and mechanical loading $\sigma_j|x|^j/a^j$ will be obtained in explicit form. Secondly, making use of the principle of superposition, the related physical quantities under thermal flux $-\sum_{i=0}^{M} Q_{0i}|x|^i/2a^{i+1}$ and mechanical loading $\sum_{j=0}^{k}\sigma_j|x|^j/a^j$ will be given explicitly. With the aid of the symmetry of thermomechanical loading, the boundary conditions under thermal flux $-Q_{0i}|x|^i/2a^{i+1}$ and mechanical loading $\sigma_j|x|^j/a^j$ are obtained.

$$\sigma_{xy}^{I}(x,0)=\sigma_{xy}^{II}(x,0)=0\ 0<x<a \tag{25}$$

$$Q_y^I(x,0)-Q_y^{II}(x,0)=-\frac{Q_{0i}-Q_{ci}}{2\mathrm{a}^{i+1}}|x|^i\ 0<x<a \tag{26}$$

$$\sigma_{yy}^{II}(x,0)=\sigma_{yy}^{I}(x,0)=\frac{\sigma_j}{a^j}|x|^j\ 0<x<a \tag{27}$$

where

$$Q_{ci}=R_c\Big(T^I(x,0)-T^{II}(x,0)\Big)+\varepsilon Q_{0i} \tag{28}$$

Furthermore, the continuity of some physical quantities meets the following relations.

$$v^{II}(x,0)=-v^I(x,0), u^{II}(x,0)=-u^I(x,0),\ x<-a\ \ or\ \ x>a \tag{29}$$

$$\sigma_{yy}^{II}(x,0)=\sigma_{yy}^{I}(x,0),\ \ \sigma_{xy}^{II}(x,0)=\sigma_{xy}^{I}(x,0),\ x<-a\ \ or\ \ x>a \tag{30}$$

$$Q_y^{II}(x,0)=Q_y^I(x,0), T^{II}(x,0)=-T^I(x,0),\ x<-a\ \ or\ \ x>a \tag{31}$$

3.1. Solution Procedure

Because Equation (14) is not directly connected to the elastic strain, the solvation of the temperature field is obtained. The expression of the temperature field is given with the help of Fourier transform.

$$T^{I,II}(x,y)=\int_0^{+\infty}\Omega^{\pm}(\xi)e^{-\xi\delta^{\pm}\lambda y}\cos(\xi x)d\xi \tag{32}$$

$\Omega^{\pm}(\xi)$, which are unknown functions, will be given. $\delta^+=1$ or $\delta^-=-1$ stands for the physical quantities of the upper or lower region of the *x*-axis. Utilizing Equation (12), one arrives at

$$Q_x^{I,II}(x,y)=\lambda_x\int_0^{+\infty}\xi\Omega^{\pm}(\xi)e^{-\xi\delta^{\pm}\lambda y}\sin(\xi x)d\xi \tag{33}$$

$$Q_y^{I,II}(x,y)=\lambda_y\lambda\int_0^{+\infty}\delta^{\pm}\xi\Omega^{\pm}(\xi)e^{-\xi\delta^{\pm}\lambda y}\cos(\xi x)d\xi \tag{34}$$

Utilizing the first expression of Equation (31), one arrives at

$$\Omega^+(\xi)=-\Omega^-(\xi), \tag{35}$$

Taking advantage of the second expressions of Equations (26) and (31) leads to

$$\int_0^{+\infty}\Omega^+(\xi)\xi\cos(\xi x)d\xi=-\frac{(Q_{0i}-Q_{ci})|x|^i}{4a^{i+1}\lambda\lambda_y}\ 0<x<a \tag{36}$$

$$\int_0^{+\infty}\Omega^+(\xi)\cos(\xi x)d\xi=0 \qquad x>a \tag{37}$$

To obtain the explicit form of Equations (36) and (37), $\gamma(x)$, which is called an auxiliary function, can be introduced

$$\gamma(x)=\frac{\partial\left[T^I(x,0)-T^{II}(x,0)\right]}{\partial x} \tag{38}$$

We have the following the expression according to the inverse Fourier transform (IFT)

$$\Omega^{+}(\xi)\xi = -\int_{0}^{a} \frac{\gamma(s)\sin(\xi s)}{\pi} ds \tag{39}$$

Inserting Equation (39) into Equation (36), one obtains

$$\frac{2}{\pi}\int_{0}^{a} \gamma(s)ds \int_{0}^{+\infty} \sin(\xi s)\cos(\xi s) = \frac{(Q_{0i} - Q_{ci})|x|^{i}}{2a^{i+1}\lambda\lambda_{y}} \tag{40}$$

Utilizing the known result [25],

$$2\int_{0}^{+\infty} \sin(\xi s)\cos(\xi s) = \frac{1}{s-x} + \frac{1}{s+x} \tag{41}$$

when $i = 2n$ ($n \geq 0$). Equation (32) can be given as

$$\frac{1}{\pi}\int_{-a}^{a} \gamma(s)\frac{1}{s-x}ds = \frac{(Q_{02n} - Q_{c2n})x^{2n}}{2a^{2n+1}\lambda\lambda_{y}} \tag{42}$$

Utilizing standard singular integral theory containing the Cauchy kernel [26], the explicit form of Equation (42) is obtained as

$$\gamma(x) = \frac{1}{\pi\sqrt{a^2 - x^2}}\int_{-a}^{a} \frac{\sqrt{a^2 - s^2}}{x-s}\frac{(Q_{02n} - Q_{c2n})s^{2n}}{2a^{2n+1}\lambda\lambda_{y}}ds + \frac{C_{2n}}{\sqrt{a^2 - x^2}} \tag{43}$$

Based on the following condition,

$$\int_{-a}^{a} \gamma(s)ds = 0 \tag{44}$$

After some calculations, one has $C_{2n} = 0$. Furthermore, $\gamma(x)$ is given as

$$\gamma(x) = \frac{(Q_{02n} - Q_{c2n})x}{2a\lambda\lambda_{y}\sqrt{a^2 - x^2}} \qquad n = 0 \tag{45}$$

$$\gamma(x) = -\sum_{l=1}^{n} \frac{(Q_{02n} - Q_{c2n})x^{2l-1}}{2a^{2n+1}\lambda\lambda_{y}\pi\sqrt{a^2 - x^2}}M_{l} + \frac{(Q_{02n} - Q_{c2n})}{2a^{2n+1}\lambda\lambda_{y}\sqrt{a^2 - x^2}}x^{2n+1} \quad n \geq 1 \tag{46}$$

where

$$M_{l} = \int_{-a}^{a} \sqrt{a^2 - s^2}s^{2n-2l}ds \ (1 \leq l \leq n) \tag{47}$$

When $i = 2n - 1$ ($n \geq 1$), Equation (40) can be rewritten as

$$\frac{1}{\pi}\int_{0}^{a} \gamma(s)\frac{2s}{s^2 - x^2}ds = \frac{(Q_{02n-1} - Q_{c2n-1})x^{2n-1}}{2a^{2n}\lambda\lambda_{y}} \tag{48}$$

Then, by the introduction of $s^2 = \bar{s}, x^2 = \bar{x}, 2sds = d\bar{s}, a^2 = \bar{a}$ and $\bar{\gamma}(\bar{s}) = \gamma(s)$, Equation (48) is expressed as

$$\frac{1}{\pi}\int_{0}^{\bar{a}} \frac{\bar{\gamma}(\bar{s})}{\bar{s} - \bar{x}}d\bar{s} = \frac{(Q_{02n-1} - Q_{c2n-1})\bar{x}^{n-\frac{1}{2}}}{2a^{2n}\lambda\lambda_{y}} \tag{49}$$

Based on a standard integral theory containing the Cauchy kernel [26], the closed form of Equation (49) is obtained as

$$\bar{\gamma}(\bar{x}) = \frac{1}{\pi\sqrt{\bar{x}(\bar{a} - \bar{x})}}\int_{0}^{\bar{a}} \frac{\sqrt{\bar{s}(\bar{a} - \bar{s})}}{\bar{x} - \bar{s}}\frac{(Q_{02n-1} - Q_{c2n-1})\bar{s}^{n-\frac{1}{2}}}{2a^{2n}\lambda\lambda_{y}}d\bar{s} \tag{50}$$

When $i = 2n$ $(n \geq 0)$, the temperature difference on the crack is obtained based on Equations (38), (45) and (46).

$$T^I(x,0) - T^{II}(x,0) = -\frac{(Q_{02n} - Q_{c2n})}{2a\lambda\lambda_y}\sqrt{a^2 - x^2} \qquad n = 0 \tag{51}$$

$$\begin{aligned} T^I(x,0) - T^{II}(x,0) &= -\sum_{l=1}^{n} \frac{(Q_{02n}-Q_{c2n})M_l}{2a^{2n+1}\lambda\lambda_y\pi} \int_{-a}^{x} \frac{s^{2l-1}}{\sqrt{a^2-s^2}}ds + \frac{(Q_{02n}-Q_{c2n})}{2a^{2n+1}\lambda\lambda_y} \int_{-a}^{x} \frac{s^{2n+1}}{\sqrt{a^2-s^2}}ds \\ &= -\sum_{l=1}^{n} \frac{(Q_{02n}-Q_{c2n})M_l}{2a^{2n+1}\lambda\lambda_y\pi} V(x,l) + \frac{(Q_{02n}-Q_{c2n})}{2a^{2n+1}\lambda\lambda_y} L(x,n) \quad n \geq 1 \end{aligned} \tag{52}$$

where

$$V(x,l) = \sqrt{a^2 - x^2}l = 1 \tag{53}$$

With the trigonometric substitution of variable s in Equation (52) and then with the help of the integral handbook [25], the following two equations can be obtained:

$$V(x,l) = -\frac{a^{2l-2}\sqrt{a^2-x^2}}{2l-1}\left[\left(\frac{x}{a}\right)^{2l-2} + \sum_{k=0}^{l-2} \frac{2^{k+1}(l-1)(l-2)\ldots(l-k-1)}{(2l-3)(2l-5)\ldots(2l-2k-3)}\left(\frac{x}{a}\right)^{2l-2k-4}\right] l \geq 2 \tag{54}$$

$$L(x,n) = -\frac{a^{2n}\sqrt{a^2-x^2}}{2n+1}\left[\left(\frac{x}{a}\right)^{2n} + \sum_{k=0}^{n-1} \frac{2^{k+1}n(n-1)(n-2)\ldots(n-k)}{(2n-1)(2n-3)(2n-5)\ldots(2n-2k-1)}\left(\frac{x}{a}\right)^{2n-2k-2}\right] n \geq 1 \tag{55}$$

When $i = 2n - 1$ $(n \geq 1)$, the temperature difference on the crack is obtained, based on Equations (38) and (50).

$$T^I(x,0) - T^{II}(x,0) = \int_0^{\overline{x}} \frac{\overline{\gamma}(\overline{s})}{2\sqrt{\overline{s}}} d\overline{s} \tag{56}$$

3.2. Elastic Field

For the solvation of Equations (9) and (10), $u^{I,II}(x,0)$ and $v^{I,II}(x,0)$ are depicted based on [26].

$$u^{I,II}(x,0) = u_1^{I,II}(x,0) + u_2^{I,II}(x,0),\ v^{I,II}(x,0) = v_1^{I,II}(x,0) + v_2^{I,II}(x,0) \tag{57}$$

Herein, the terms of $u_1^{I,II}(x,0)$ and $v_1^{I,II}(x,0)$, respectively, correspond to the general solution under a certain heat flow, and $u_2^{I,II}(x,0)$ and $v_2^{I,II}(x,0)$, respectively, correspond to the special solution under a certain temperature field. We can see $u_1^{I,II}(x,0)$ and $v_1^{I,II}(x,0)$ are expressed based on the Fourier transform.

$$u_1^{I,II}(x,0) = \sum_{j=1}^{2} \int_0^{+\infty} \Omega_j^{\pm}(\xi)\sin(\xi x)d\xi \tag{58}$$

$$v_1^{I,II}(x,0) = \sum_{j=1}^{2} \int_0^{+\infty} \eta_j\delta^{\pm}\Omega_j^{\pm}(\xi)\cos(\xi x)d\xi \tag{59}$$

where $\Omega_j^{\pm}(\xi)(j = 1,2)$ are unknown functions. $\gamma_j(j = 1,2)$ are given in the following equations.

$$c_{22}c_{66}\gamma^4 + \left(c_{12}^2 + 2c_{12}c_{66} - c_{12}c_{22}\right)\gamma^2 + c_{11}c_{66} = 0 \tag{60}$$

where

$$\eta_j = \frac{c_{11} - c_{66}\gamma_j^2}{(c_{12} + c_{66})\gamma_j} \tag{61}$$

Furthermore, $u_2^{I,II}(x,0)$ and $v_2^{I,II}(x,0)$ are selected as

$$u_2^{I,II}(x,0) = \sum_{j=1}^{2} \int_0^{+\infty} \Omega *^{\pm}(\xi)\sin(\xi x)d\xi \tag{62}$$

$$v_2^{I,II}(x,0) = \sum_{j=1}^{2} \int_0^{+\infty} \delta^{\pm} L*^{\pm}(\xi)\cos(\xi x)d\xi \tag{63}$$

Substituting Equations (62) and (63) for Equations (8) and (9), one has

$$\begin{bmatrix} \Omega*^{\pm}(\xi) \\ L*^{\pm}(\xi) \end{bmatrix} = \begin{bmatrix} K_1 \\ K_2 \end{bmatrix} \frac{\Omega^{+}(\xi)}{\xi} \tag{64}$$

where

$$\begin{bmatrix} K_1 \\ K_2 \end{bmatrix} = \begin{bmatrix} c_{11} - c_{66}\lambda^2 & -(c_{12}+c_{66})\lambda \\ (c_{12}+c_{66})\lambda & c_{66} - c_{22}\lambda^2 \end{bmatrix}^{-1} \begin{bmatrix} \beta_1 \\ \beta_2\lambda \end{bmatrix} \tag{65}$$

The components of stress are expressed in the following form with the application of Equations (2)–(4), (51)–(59).

$$\begin{aligned} \sigma_{xx}^{I,II}(x,0) = \textstyle\sum_{j=1}^{2} \int_0^{+\infty} (c_{11} - c_{12}\gamma_j\eta_j)\xi\Omega_j^{\pm}(\xi)\cos(\xi x)d\xi \\ +(c_{11}K_1 - c_{12}\lambda K_2 - \beta_1)\int_0^{+\infty}\Omega^{\pm}(\xi)\cos(\xi x)d\xi \end{aligned} \tag{66}$$

$$\begin{aligned} \sigma_{yy}^{I,II}(x,0) = \textstyle\sum_{j=1}^{2} \int_0^{+\infty} (c_{12} - c_{22}\gamma_j\eta_j)\xi\Omega_j^{\pm}(\xi)\cos(\xi x)d\xi \\ +(c_{12}K_1 - c_{22}\lambda K_2 - \beta_2)\int_0^{+\infty}\Omega^{\pm}(\xi)\cos(\xi x)d\xi \end{aligned} \tag{67}$$

$$\begin{aligned} \sigma_{xy}^{I,II}(x,0) = -c_{66}\Big[\textstyle\sum_{j=1}^{2} \int_0^{+\infty} \delta^{\pm}(\gamma_j+\eta_j)\xi\Omega_j^{\pm}(\xi)\sin(\xi x)d\xi \\ +\int_0^{+\infty}\delta^{\pm}(K_1\lambda + K_2)\Omega^{\pm}(\xi)\sin(\xi x)d\xi\Big] \end{aligned} \tag{68}$$

To obtain the closed form of this problem, it is separated into two simple sections. One is mechanical loading $\sigma_j|x|^j/a^j$, the other is thermal loading $-Q_{0i}|x|^i/2a^{i+1}$. To begin with, dual integral equations can be given, considering the mechanical loading.

$$\sigma_{xy}^{I}(x,0) = \sigma_{xy}^{II}(x,0) = 0 \quad x > 0 \tag{69}$$

$$v^{I}(x,0) = -v^{II}(x,0) = 0 \quad x > a \tag{70}$$

Making use of Equations (69) and (70), one has

$$\Omega_j^{+}(\xi) = \Omega_j^{-}(\xi),\ \Omega_2^{+}(\xi) = -\frac{\gamma_1+\eta_1}{\gamma_2+\eta_2}\Omega_1^{+}(\xi) \tag{71}$$

With application of Equations (18) and (54), one attains

$$\int_0^{+\infty} \xi\Omega_1^{+}(\xi)\cos(\xi x)d\xi = \frac{\sigma_j|x|^j}{\omega_1 a^j} \quad 0 < x < a \tag{72}$$

$$\int_0^{+\infty} \xi\Omega_1^{+}(\xi)\cos(\xi x)d\xi = 0 \quad x > a \tag{73}$$

where

$$\omega_1 = (c_{12} - c_{22}\gamma_1\eta_1) - \frac{\gamma_1+\eta_1}{\gamma_2+\eta_2}(c_{12} - c_{22}\gamma_2\eta_2) \tag{74}$$

To achieve the closed form of Equations (72) and (73), the called auxiliary function $\phi(x)$ is introduced as

$$\phi(x) = \frac{\partial v^{I}(x,0)}{\partial x} \tag{75}$$

Making use of inverse Fourier transform (IFT) leads to

$$\Omega_1^{+}(\xi)\xi = -\frac{2(\gamma_2+\eta_2)}{(\eta_1\gamma_2 - \eta_2\gamma_1)\pi}\int_0^{a}\phi(s)\sin(\xi s)ds \tag{76}$$

Taking advantage of Equation (41) and substituting Equation (76) into (73), one has

$$\frac{1}{\pi}\int_{-a}^{a}\frac{\phi(s)}{s-x}ds=-\frac{\sigma_j(\eta_1\gamma_2-\eta_2\gamma_1)}{\omega_1(\gamma_2+\eta_2)a^j}|x|^j \tag{77}$$

When $j = 2n$ ($n \geq 0$), the solution of Equation (77) can be obtained with the application of the standard singular integral containing the Cauchy kernel [26].

$$\phi(x)=-\frac{1}{\pi\sqrt{a^2-x^2}}\int_{-a}^{a}\frac{\sqrt{a^2-s^2}}{x-s}\frac{\sigma_{2n}(\eta_1\gamma_2-\eta_2\gamma_1)}{\omega_1(\gamma_2+\eta_2)a^{2n}}s^{2n}ds+\frac{D_{2n}}{\sqrt{a^2-x^2}} \tag{78}$$

After some calculations, $D_{2n}=0$. Utilizing Equations (75) and (78), the elastic displacement is obtained as

$$v^I(x,0)=\frac{\sigma_{2n}(\eta_1\gamma_2-\eta_2\gamma_1)\sqrt{a^2-x^2}}{\omega_1(\gamma_2+\eta_2)} \quad n=0 \tag{79}$$

$$\begin{aligned} v^I(x,0) &= \sum_{l=1}^{n}\frac{\sigma_{2n}(\eta_1\gamma_2-\eta_2\gamma_1)M_l}{\omega_1(\gamma_2+\eta_2)\pi a^{2n}}\int_{-a}^{x}\frac{s^{2l-1}}{\sqrt{a^2-s^2}}ds-\frac{\sigma_{2n}(\eta_1\gamma_2-\eta_2\gamma_1)}{\omega_1(\gamma_2+\eta_2)a^{2n}}\int_{-a}^{x}\frac{s^{2n+1}}{\sqrt{a^2-s^2}}ds \\ &= \sum_{l=1}^{n}\frac{\sigma_{2n}(\eta_1\gamma_2-\eta_2\gamma_1)M_l}{\omega_1(\gamma_2+\eta_2)\pi a^{2n}}V(x,l)-\frac{\sigma_{2n}(\eta_1\gamma_2-\eta_2\gamma_1)}{\omega_1(\gamma_2+\eta_2)a^{2n}}L(x,n) \quad n\geq 1 \end{aligned} \tag{80}$$

Inserting Equation (78) into (67), the stress field is given as

$$\sigma_{yy}^{I,II}(x,0)=-\left(1-\frac{x}{\sqrt{x^2-a^2}}\right)\sigma_{2n} \; n=0 \tag{81}$$

$$\begin{aligned} \sigma_{yy}^{I,II}(x,0) &= \sum_{l=1}^{n}\frac{\sigma_{2n}}{a^{2n}\pi^2}\int_{-a}^{a}\frac{s^{2l-1}}{(s-x)\sqrt{a^2-s^2}}ds-\frac{\sigma_{2n}}{a^{2n}\pi}\int_{-a}^{a}\frac{s^{2n+1}}{(s-x)\sqrt{a^2-s^2}}ds \\ &= \sum_{l=1}^{n}\left[M(l,x)M_l-\frac{x^{2l-1}\pi}{\sqrt{x^2-a^2}}M_l\right]\frac{\sigma_{2n}}{a^{2n}\pi^2}-\left[N(n,x)-\frac{x^{2n+1}\pi}{\sqrt{x^2-a^2}}\right]\frac{\sigma_{2n}}{a^{2n}\pi} \; n\geq 1 \end{aligned} \tag{82}$$

where

$$M(l,x)=\sum_{m=0}^{l-1}Z_m x^{2m}, N(n,x)=\sum_{m=0}^{n}W_m x^{2m} \tag{83}$$

$$Z_m=\int_{-a}^{a}\frac{s^{2l-2\mathrm{m}-2}}{\sqrt{a^2-s^2}}ds(0\leq m\leq l-1),\; W_m=\int_{-a}^{a}\frac{s^{2n-2\mathrm{m}}}{\sqrt{a^2-s^2}}ds\;(0\leq m\leq n) \tag{84}$$

When $j = 2n - 1$ ($n \geq 1$), Equation (77) can be rewritten as

$$\frac{1}{\pi}\int_{0}^{a}\phi(s)\frac{2s}{s^2-x^2}ds=-\frac{\sigma_{2n-1}(\eta_1\gamma_2-\eta_2\gamma_1)}{\omega_1(\gamma_2+\eta_2)a^{2n-1}}x^{2n-1} \tag{85}$$

Then, utilizing the introduction of $s^2=\bar{s}$, $x^2=\bar{x}$, $2sds=d\bar{s}$, $a^2=\bar{a}$, Equation (85) is also expressed as

$$\frac{1}{\pi}\int_{0}^{\bar{a}}\frac{\bar{\phi}(\bar{s})}{\bar{s}-\bar{x}}d\bar{s}=-\frac{\sigma_{2n-1}(\eta_1\gamma_2-\eta_2\gamma_1)}{\omega_1(\gamma_2+\eta_2)a^{2n-1}}\bar{x}^{n-\frac{1}{2}} \tag{86}$$

Utilizing standard singular integral theory containing the Cauchy kernel [26], the explicit form of Equation (86) is obtained as

$$\bar{\phi}(\bar{x})=-\frac{1}{\pi\sqrt{\bar{x}(\bar{a}-\bar{x})}}\int_{0}^{\bar{a}}\frac{\sqrt{\bar{s}(\bar{a}-\bar{s})}}{\bar{x}-\bar{s}}\frac{\sigma_{2n-1}(\eta_1\gamma_2-\eta_2\gamma_1)}{\omega_1(\gamma_2+\eta_2)a^{2n-1}}\bar{s}^{n-\frac{1}{2}}d\bar{s} \tag{87}$$

Based on the following constraint condition, one has

$$\frac{1}{2}\int_{0}^{\bar{a}}\frac{\bar{\phi}(\bar{s})}{\sqrt{\bar{s}}}d\bar{s}=0 \tag{88}$$

Based on Equations (75) and (87), the elastic displacement is obtained as

$$v^I(x,0) = \frac{1}{2}\int_0^{\overline{x}} \frac{\overline{\phi}(\overline{s})}{\sqrt{\overline{s}}} d\overline{s} \tag{89}$$

After some computations, one has

$$v^I(x,0) = \frac{\sigma_{2n-1}(\eta_1\gamma_2 - \eta_2\gamma_1)x\sqrt{a^2 - x^2}}{2\pi a\omega_1(\gamma_2 + \eta_2)} + O(1) \quad n = 1 \tag{90}$$

$$v^I(x,0) = \sum_{l=1}^{n} \frac{\sigma_{2n-1}(\eta_1\gamma_2 - \eta_2\gamma_1)M'_l}{2\omega_1(\gamma_2 + \eta_2)\pi a^{2n-1}} \int_0^{\overline{x}} \frac{\overline{s}^{l-1}}{\sqrt{\overline{s}(\overline{a} - \overline{s})}} d\overline{s} - \frac{\sigma_{2n-1}(\eta_1\gamma_2 - \eta_2\gamma_1)}{\omega_1(\gamma_2 + \eta_2)\pi a^{2n-2}} \int_0^{\overline{x}} \frac{\overline{s}^{n-1}}{\sqrt{\overline{s}(\overline{a} - \overline{s})}} d\overline{s} + O(1), n \geq 2 \tag{91}$$

where

$$M'_l = \int_0^{\overline{a}} \sqrt{\overline{a} - \overline{s}}\,\overline{s}^{n-l} d\overline{s} \ (1 \leq l \leq n) \tag{92}$$

Substituting Equation (87) into (67), the stress field is given

$$\sigma_{yy}^{I,II}(x,0) = \frac{2x}{\pi a\sqrt{x^2 - a^2}}\sigma_{2n-1} + O(1) \ n = 1 \tag{93}$$

$$\sigma_{yy}^{I,II}(x,0) = \sum_{l=1}^{n} \frac{\sigma_{2n-1}M'_l}{\pi^2 a^{2n-1}} \int_0^{\overline{a}} \frac{\overline{s}^{l-1}}{(\overline{s} - \overline{x})\sqrt{\overline{s}(\overline{a} - \overline{s})}} d\overline{s} - \frac{\sigma_{2n-1}}{\pi^2 a^{2n-2}} \int_0^{\overline{a}} \frac{\overline{s}^{n-1}}{(\overline{s} - \overline{x})\sqrt{\overline{s}(\overline{a} - \overline{s})}} d\overline{s} + O(1), \ n \geq 2 \tag{94}$$

Next, an elastic field with thermal flux $\left(-Q_{0i}|x|^i/2a^{i+1}\right)$ will be solved. Using thermal flux, one has the relation

$$\sigma_{yy}^{I}(x,0) = \sigma_{yy}^{II}(x,0) = 0 \ \ 0 < x < a \tag{95}$$

Taking advantage of Equations (67) and (95), one obtains

$$\Omega_j^+(\xi) = -\Omega_j^-(\xi) \tag{96}$$

$$\sum_{j=1}^{2}(c_{12} - c_{22}\gamma_j\eta_j)\Omega_j^+(\xi) = (c_{22}\lambda K_2 + \beta_2 - c_{12}K_1)\frac{\Omega^+(\xi)}{\xi} \tag{97}$$

Applying Equation (25) and the second expression in Equation (29), one has dual integral equations

$$\int_0^{+\infty} \sum_{j=1}^{2}(\gamma_j + \eta_j)\xi\Omega_j^+(\xi)\sin(\xi x)d\xi + \int_0^{+\infty}(K_1\lambda + K_2)\Omega^+(\xi)\sin(\xi x)d\xi = 0, \ 0 < x < a \tag{98}$$

$$\int_0^{+\infty}\left[\sum_{j=1}^{2}\Omega_j^+(\xi)\sin(\xi x) + \frac{K_1\Omega^+(\xi)}{\xi}\sin(\xi x)\right]d\xi = 0, \ x > a \tag{99}$$

To get the explicit form of Equations (98) and (99), the called auxiliary function is also introduced as

$$\Theta(x) = \frac{\partial u^I(x,0)}{\partial x} \tag{100}$$

Making use of Equation (98) and inverse Fourier transform, we have

$$\sum_{j=1}^{2}\Omega_j^+(\xi)\xi + K_1\Omega^+(\xi) = \frac{2}{\pi}\int_0^a \Theta(s)\cos(\xi s)ds \tag{101}$$

With the application of Equations (97) and (101), one arrives at

$$\Omega_1^+(\xi)\xi = \frac{c_{22}\lambda K_2 + \beta_2 - c_{22}\gamma_2\eta_2 K_1}{c_{22}(\gamma_2\eta_2 - \gamma_1\eta_1)}\Omega^+(\xi) + \frac{c_{22}\gamma_2\eta_2 - c_{12}}{c_{22}(\gamma_2\eta_2 - \gamma_1\eta_1)}\frac{2}{\pi}\int_0^a \Theta(s)\cos(\xi s)ds \tag{102}$$

$$\Omega_2^+(\xi)\xi = \frac{c_{22}\gamma_1\eta_1 K_1 - c_{22}\lambda K_2 - \beta_2}{c_{22}(\gamma_2\eta_2 - \gamma_1\eta_1)}\Omega^+(\xi) + \frac{c_{12} - c_{22}\gamma_1\eta_1}{c_{22}(\gamma_2\eta_2 - \gamma_1\eta_1)}\frac{2}{\pi}\int_0^a \Theta(s)\cos(\xi s)ds \tag{103}$$

With the application of Equations (99), (102), and (103), one has

$$2\int_0^a \Theta(s)ds\int_0^{+\infty}\sin(\xi x)\cos(\xi s)d\xi = \pi\omega_2\int_0^{+\infty}\Omega^+(\xi)\sin(\xi x)d\xi,\ 0 < x < a \tag{104}$$

where

$$\omega_2 = \frac{H_1}{H_2} \tag{105}$$

with

$$\begin{aligned} H_1 &= (\gamma_1 + \eta_1)(c_{22}\gamma_2\eta_2 K_1 - c_{22}\lambda K_2 - \beta_2) + (\gamma_2 + \eta_2) \\ &\times(c_{22}\lambda K_2 + \beta_2 - c_{22}\gamma_1\eta_1 K_1) + c_{22}(K_1\lambda + K_2)(\gamma_1\eta_1 - \gamma_2\eta_2) \end{aligned} \tag{106}$$

$$H_2 = (\gamma_1 + \eta_1)(c_{22}\gamma_2\eta_2 - c_{12}) + (\gamma_2 + \eta_2)(c_{12} - c_{22}\gamma_1\eta_1) \tag{107}$$

When $i = 2n$ ($n \geq 0$), applying Equation (41), Equation (104) is given

$$\frac{1}{\pi}\int_{-a}^a \frac{\Theta(s)}{x - s}ds = \omega_2\int_0^{+\infty}\Omega^+(\xi)\sin(\xi x)d\xi \tag{108}$$

Utilizing the inverse Fourier transform of Equation (32) and the known result of Equation (41), one has

$$\int_0^{+\infty}\Omega^+(\xi)\sin(\xi x)d\xi = \frac{1}{\pi}\int_{-a}^a \frac{T^+(s) - T^-(s)}{x - s}ds \tag{109}$$

Based on Equations (51) and (52), Equation (109) is given as

$$\int_0^{+\infty}\Omega^+(\xi)\sin(\xi x)d\xi = -\frac{Q_{02n} - Q_{c2n}}{a\lambda\lambda_y}x, \tag{110}$$

$$\int_0^{+\infty}\Omega^+(\xi)\sin(\xi x)d\xi = -\sum\nolimits_{l=1}^n \frac{(Q_{02n} - Q_{c2n})M_l}{2a\lambda\lambda_y(2l-1)\pi^2}T(x,l) + \frac{Q_{02n} - Q_{c2n}}{2a^{2n+1}(2n+1)\lambda\lambda_y\pi}(x,n),\ n \geq 1 \tag{111}$$

where

$$T(x,l) = x\pi, \qquad l = 1 \tag{112}$$

$$T(x,l) = [\left(\sum\nolimits_{p=1}^l x^{2p-1}I_p + x^{2l-1}\pi\right) + a^{2k+2}\sum\nolimits_{k=0}^{l-2}\frac{2^{k+1}(l-1)(l-2)\ldots(l-k-1)}{(2l-3)(2l-5)\ldots(2l-2k-3)} \times \left[\left(A_1 x + \ldots + x^{2l-2\mathrm{k}-3}\pi\right)\right],\ \ l \geq 2 \tag{113}$$

$$(x,n) = \left[\sum\nolimits_{p=1}^i (x^{2p-1}J_p + x^{2n+1}\pi\right) + a^{2k+2}\sum\nolimits_{k=0}^{n-1}\frac{2^{k+1}n(n-1)(n-2)\ldots(n-k)}{(2n-1)(2n-3)(2n-5)\ldots(2n-2k-1)} \times \left(B_1 x + .. + x^{2n-2\mathrm{k}-1}\pi\right)],\ \ n \geq 1 \tag{114}$$

$$I_p = -\int_{-a}^a \sqrt{a^2 - s^2}s^{2l-2p-2}ds\ ,\ (1 \leq p \leq l-1) \tag{115}$$

$$A_j = -\int_{-a}^a \sqrt{a^2 - s^2}s^{2l-2k-4-2j}ds,\ (1 \leq j \leq l-k-2) \tag{116}$$

$$J_p = -\int_{-a}^a \sqrt{a^2 - s^2}s^{2n-2p}ds,\ (1 \leq p \leq l) \tag{117}$$

$$B_j = -\int_{-a}^a \sqrt{a^2 - s^2}s^{2n-2k-2-2j}ds,\ (1 \leq j \leq n-k-1) \tag{118}$$

Utilizing the singular integral containing the Cauchy kernel [26], the closed form of the solution can be given as

$$\Theta(x) = \frac{\omega_2}{\pi^2\sqrt{a^2-x^2}} \int_{-a}^{a} \frac{\sqrt{a^2-s^2}}{x-s} [\textstyle\sum_{l=1}^{n} \frac{(Q_{02n}-Q_{c2n})M_l}{2a\lambda\lambda_y(2l-1)\pi} T(l,s) - \frac{(Q_{02n}-Q_{c2n})}{2a^{2n+1}(2n+1)\lambda\lambda_y}(s,n)]ds \tag{119}$$

With the knowledge of Equation (100), one has

$$u^I(x,0) = \int_{-a}^{x} \Theta(s)ds \tag{120}$$

Based on Equations (68), (102), (103), and (119), the shearing stresses are obtained as

$$\sigma_{xy}^{I,II}(x,0) = \frac{c_{66}}{\pi c_{22}(\gamma_2\eta_2-\gamma_1\eta_1)}\{H_2\int_{-a}^{a}\frac{\Theta(s)}{x-s}ds - H_1[\textstyle\sum_{l=1}^{n}\frac{(Q_{02n}-Q_{c2n})M_l}{2a\lambda\lambda_y(2l-1)\pi^2}T(x,l) - \frac{(Q_{02n}-Q_{c2n})}{2a^{2n+1}(2n+1)\lambda\lambda_y\pi}(x,n)]\} \tag{121}$$

When $i = 2n - 1$ ($n \geq 1$), one gets from Equation (39)

$$\begin{aligned}\textstyle\int_0^{+\infty}\Omega^+(\xi)\sin(\xi x)d\xi &= -\tfrac{2}{\pi}\textstyle\int_0^{+\infty}\gamma(s)d\xi\int_0^{+\infty}\frac{\sin(\xi s)\sin(\xi x)}{\xi}ds \\ &= -\tfrac{1}{\pi}\textstyle\int_0^{+\infty}\gamma(s)\ln\left|\frac{s+x}{s-x}\right|ds\end{aligned} \tag{122}$$

Based on the following result [25]:

$$\int_0^{+\infty}\frac{\sin(\xi s)\sin(\xi x)}{\xi}d\xi = \frac{1}{4}\ln\left(\frac{s+x}{s-x}\right)^2 \tag{123}$$

Utilizing Equation (122), Equation (104) can be calculated as

$$\frac{1}{\pi}\int_0^{\overline{a}}\frac{\overline{\Theta}(\overline{s})}{(\overline{s}-\overline{x})\sqrt{\overline{s}}}d\overline{s} = \omega_2\int_0^{+\infty}\Omega^+(\xi)\sin(\xi x)d\xi,\ \ 0<x<a \tag{124}$$

Utilizing the standard singular integral containing the Cauchy kernel [26], the explicit form of the solution is obtained as

$$\frac{\overline{\Theta}(\overline{x})}{\sqrt{\overline{x}}} = \frac{\omega_2(Q_{02n-1}-Q_{c2n-1})}{\pi\lambda\lambda_y\sqrt{\overline{x}(\overline{a}-\overline{x})}}\int_0^{\overline{a}}\frac{\sqrt{\overline{s}(\overline{a}-\overline{s})}}{\overline{x}-\overline{s}}d\overline{s}\int_0^{+\infty}\Omega^+(\xi)\sin(\xi x)d\xi \tag{125}$$

Based on Equation (100), one has

$$u(x,0) = \frac{1}{2}\int_0^{\overline{x}}\frac{\overline{\Theta}(\overline{s})}{\sqrt{\overline{s}}}d\overline{s} \tag{126}$$

According to Equations (68), (102), (103), and (125), one obtains

$$\sigma_{xy}^{I,II}(x,0) = \frac{c_{66}}{\pi c_{22}(\gamma_2\eta_2-\gamma_1\eta_1)}\int_0^a\left[\frac{2H_2x\Theta(s)}{s^2-x^2} - H_1\gamma(s)\ln\left|\frac{s+x}{s-x}\right|\right]ds \tag{127}$$

Utilizing superposition theory, a physical quantity under symmetrical thermal flux $-\sum_{i=0}^{M}Q_{0i}|x|^i/2a^{i+1}$ and mechanical loading $\sum_{j=0}^{k}\sigma_j|x|^j/a^j$ can be obtained in closed forms.

4. Fracture Parameters

It is of great significance for the stress intensity factor (SIF) to characterize the stress field of the crack tip, and the corresponding mode-I and mode II stress intensity factors are defined [27].

$$K_I = \lim_{x\to a^+}\sqrt{2\pi(x-a)}\sigma_{yy}^{I,II}(x,0) \tag{128}$$

$$K_{II} = \lim_{x \to a^+} \sqrt{2\pi(x-a)}\sigma_{xy}^{I,II}(x,0) \tag{129}$$

Next, the corresponding intensity factors for the characterization of a single crack displacement are given as

$$K_v^{COD} = \lim_{x \to a^+} \sqrt{\frac{\pi}{2(a-x)}} v^I(x,0) \tag{130}$$

$$K_u^{COD} = \lim_{x \to a^+} \sqrt{\frac{\pi}{2(a-x)}} u^I(x,0) \tag{131}$$

The energy release rate G, which is of much significance on the characterization of crack growth, is defined as [28].

$$G = \lim_{\delta \to 0} \frac{1}{\delta} \int_0^\delta \sigma_{yy}^I(x+a,0)v^I(a-x,0) + \sigma_{xy}^I(x+a,0)u^I(a-x,0)dx \tag{132}$$

The energy density dW/dV, which is of much importance on the characterization of mechanics, is expressed as follows for a non-iso-thermal problem [2,3].

$$\frac{dW}{dV} = \frac{S}{r} = \frac{1}{2}\sigma_{mn}\varepsilon_{mn} - \frac{1}{2}\alpha_{kk}T\sigma_{kk} \tag{133}$$

where S and r denote the strain energy density factor and the reach to the crack tip, respectively. About the solid, which is regarded to be orthotropic, the strain energy can also be given by utilizing the previous equation.

$$\frac{S}{r} = \frac{c_{22}(\sigma_{xx}^I)^2 + c_{11}(\sigma_{yy}^I)^2 - 2c_{12}\sigma_{xx}^I\sigma_{yy}^I}{2c_{11}c_{22} - c_{12}^2} + \frac{(\sigma_{xy}^I)^2}{2c_{66}} \tag{134}$$

5. Numerical Results

Some numerical examples are selected to address the effect of ϖ_c and ε on the physical quantity, and fracture parameters. Yet the general, the thermal flux, and mechanical loading are selected as quadratic thermo-mechanical flux ($-(Q_{02} - Q_{c2})x^2/2a^3$ and $\sigma_2 x^2/a^2$). K_{II2}, G_2, and S_2 stand for the fracture parameters, respectively, under thermo-mechanical flux $-(Q_{02} - Q_{c2})x^2/2a^3$ and $\sigma_2 x^2/a^2$. The dimensionless thermal conductivity $\varpi_c = R_c/\lambda_y$ is defined for the sake of simplicity. The orthotropic material is selected as shown in [29] (Table 1).

Table 1. Tyrannohex.

E_{xx} (MPa)	E_{yy} (MPa)	G_{xy} (MPa)	v_{xy}	v_{yx}	α_{xx} (10^{-6}/°C)	α_{yy} (10^{-6}/°C)	λ_x (w/m°C)	λ_y (w/m°C)
135,000	87,000	50,000	0.15	0.09667	3.2	3.2	3.08	2.81

Figure 2 shows Q_{c2}/Q_{02} versus ϖ_c with ε = 0.01 and x/a =0, 0.25, 0.5, 0.75. It is easily found that Q_{c2}/Q_{02} increases as ϖ_c increases for ε = 0.01. When ϖ_c = 0 and ε = 0, one has $Q_{c2} = 0$, which corresponds to a fully impermeable case. When $\varpi_c \to \infty$, one has $Q_{c2} = Q_{02}$, which means a fully permeable case. In addition to the case of epsilon = 0.01 shown in Figure 2, two cases of epsilon = 0.005 and 0.02 are also calculated, and the results show that they have little difference from the case of epsilon = 0.01. It reveals that the change of epsilon only has a small effect on Q_{c2}/Q_{02}.

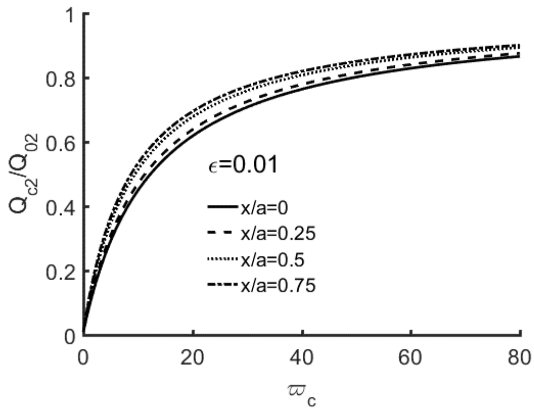

Figure 2. Q_{c2}/Q_{02} versus ϖ_c with ε = 0.01 and $x/a = 0, 0.25, 0.5, 0.75$.

Figure 3 shows Q_{c2}/Q_{02} versus ε with ϖ_c=1 and x/a =0, 0.25, 0.5, 0.75. Q_{c2}/Q_{02} is increasing as ε is rising. Based on Figures 2 and 3, the case of ϖ_c = 0 and ε = 0 or $\varpi_c \rightarrow \infty$ corresponds to a fully impermeable or permeable crack.

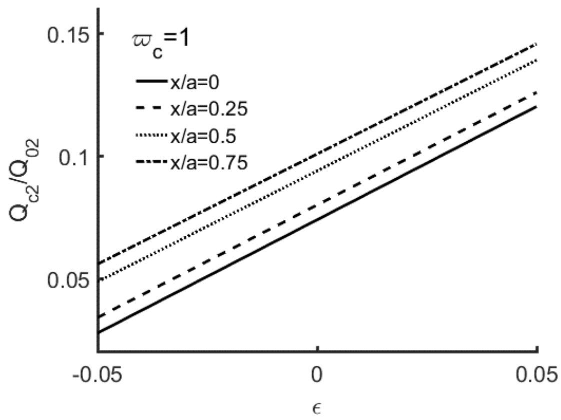

Figure 3. Q_{c2}/Q_{02} versus ε with ϖ_c = 1 and $x/a = 0, 0.25, 0.5, 0.75$.

Figure 4 displays K_{II2}/K_{II20} versus ϖ_c with $\varepsilon = 0.01$, where K_{II20} represents K_{II2} when Q_{c2} = 0 and ε = 0. K_{II2}/K_{II20} is decreasing with an increase of ϖ_c for a fixed *x/a*. Figure 5 displays K_{II2}/K_{II20} versus ε with $\varpi_c = 1$. K_{II2}/K_{II20} is decreasing as ε is rising. It is revealed that changing the properties of the materials of the crack inside (i.e., thermal conductivity) can increase or decrease the values of some physical quantities.

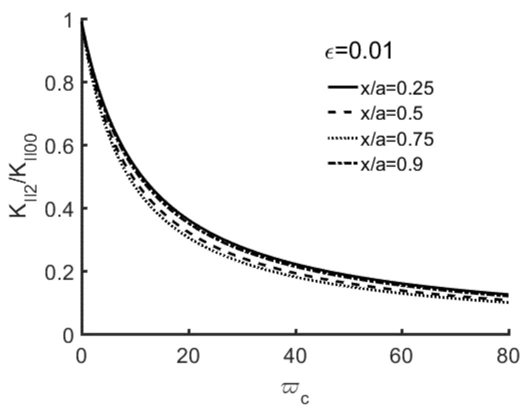

Figure 4. K_{II2}/K_{II20} versus ϖ_c with ε = 0.01 and $x/a = 0.25, 0.5, 0.75, 0.9$.

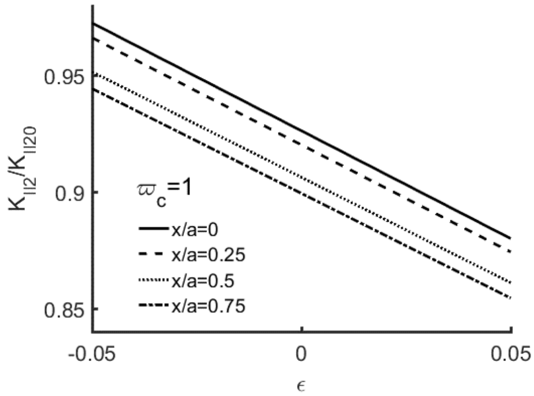

Figure 5. K_{II2}/K_{II20} versus ε with ϖ_c = 1 and $x/a = 0, 0.25, 0.5, 0.75$.

Figures 6–8 show G_2 is increasing as remote tensile stress is rising for the case of $\varpi_c = 0$ and ε = 0.01. When the relative proportion of thermal loading is especially dominant over remote tensile stress, G_2 is not positive, implying the crack is partly enclosed. The positive energy release rate will not be physically meaningful.

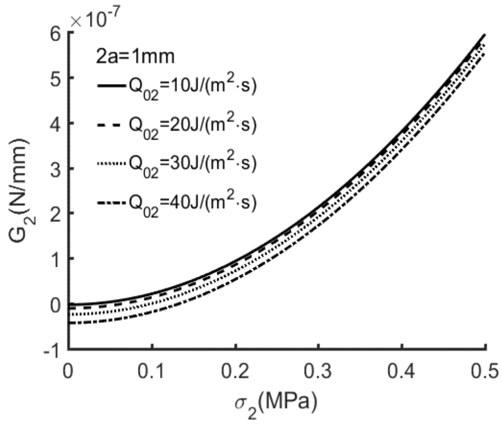

Figure 6. G_2 versus tension stress with $Q_{02} = 10, 20, 30, 40\ \mathrm{J}/(\mathrm{m}^2{\cdot}\mathrm{s})$ for $\varpi_c = 0$ and ε = 0.01. (2*a* = 1 mm).

Figures 9–11 show $S_2/(\sigma_2{}^2\pi a)$ for the case of $\varpi_c = 0$ and ε = 0.01 with a series of *r*/*a*. It is easily seen that $S_2/(\sigma_2{}^2\pi a)$ is increasing as thermal flux is rising. In any circumstance, the value of the strain energy density is not negative.

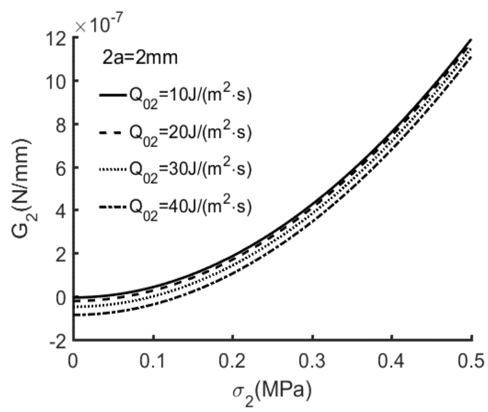

Figure 7. G_2 versus tension stress with $Q_{02} = 10, 20, 30, 40\ \mathrm{J}/(\mathrm{m}^2{\cdot}\mathrm{s})$ for $\varpi_c = 0$ and ε = 0.01. (2*a* = 2 mm).

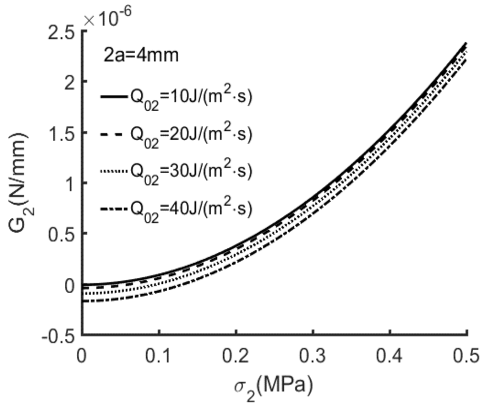

Figure 8. G_2 versus tension stress with $Q_{02} = 10,\ 20,\ 30,\ 40\ \mathrm{J}/\left(\mathrm{m}^2{\cdot}\mathrm{s}\right)$ for $\varpi_c = 0$ and $\varepsilon = 0.01$. ($2a = 4$ mm).

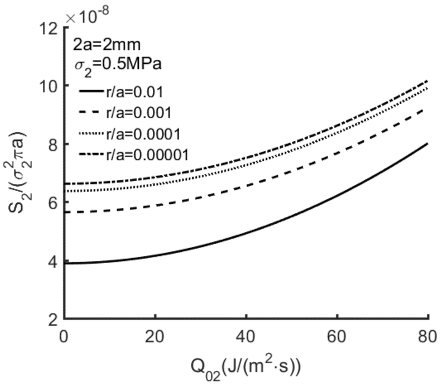

Figure 9. $S_2/(\sigma_2{}^2\pi a)$ versus Q_{02} with $r/a = 0.01,\ 0.001, 0.0001, 0.00001$ for $\varpi_c = 0$ and $\varepsilon = 0.01$. ($2a = 2$ mm, $\sigma_2 = 0.5$ MPa).

Based on the mentioned results, when $\varpi_c = 0$ and $\varepsilon = 0$ or $\varpi_c \to\infty$, it implies a fully impermeable or permeable case. Filling some material into the internal crack can reduce or increase the values of some physical quantities and fracture parameters. Therefore, the properties of the crack inside should be emphasized in the fracture behavior of bodies containing cracks. Furthermore, enough consideration should be given to crack closure as the energy release rate is applied to analyze a cracked solid.

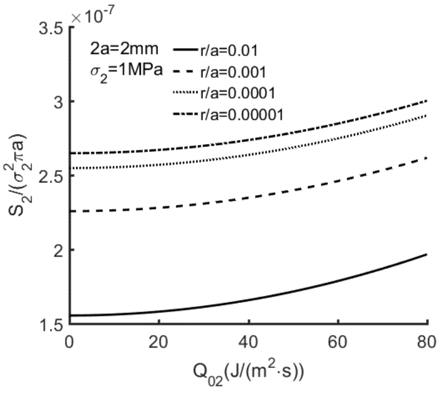

Figure 10. $S_2/(\sigma_2{}^2\pi a)$ versus Q_{02} with $r/a = 0.01, 0.001, 0.0001, 0.00001$ for $\varpi_c = 0$ and $\varepsilon = 0.01$. ($2a = 2$ mm, $\sigma_2 = 1$ MPa).

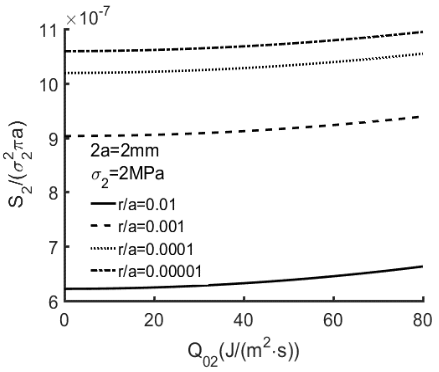

Figure 11. $S_2/(\sigma_2{}^2\pi a)$ versus Q_{02} with $r/a = 0.01, 0.001, 0.0001, 0.00001$ for ϖ_c and $\varepsilon = 0.01$. ($2a = 2$ mm, $\sigma_2 = 2$ MPa).

6. Conclusions

The thermo-elastic problem of a cracked orthotropic solid is considered under symmetrical heat flow and symmetrical mechanical loading in this paper. The raised modified partially impermeable crack model, Fourier transforms technique (FTT), and superposition theory are used to give the closed form of the correlative physical quantity. Some simple examples show that the dimensionless thermal resistance (ϖ_c) between the upper and lower crack regions and the proposed coefficient (ϵ) play an essential influence on the related physical quantities and fracture parameters and that the value of the energy release rate may be positive or negative under thermoelastic loading. Therefore, the properties of the internal crack and the energy release rate should be emphasized to assess the growth of the crack.

As the solutions obtained from this paper are explicitly closed, the calculation of the stress intensity factors of various cracks with different lengths becomes very convenient and fast. It is worth mentioning that the method provided in this paper cannot solve the fracture problems of a cracked structure with a complex shape. In addition, when using the method mentioned in this paper to solve the finite boundary crack problem, it is difficult to obtain accurate results. If you need to solve the above problem, you can use other numerical methods, such as the finite element [30], semi-analytical solutions [31], the 'Galerkin method' [32,33], and the 'Bezier method' [34,35] etc.

Author Contributions: Conceptualization, B.W. and D.P.; method-ology, B.W. and D.P.; software, B.W.; validation, B.W., D.P. and R.J.; formal analysis, B.W.; writing—original draft preparation, B.W.; writing—review and editing, D.P. and R.J. All authors have read and agreed to the published version of the manuscript.

Funding: The work was supported by the Hebei University Scientific Research Foundation for higher-level talent No:521100221019.

Conflicts of Interest: The authors declare no conflict of interest.

References

1. Nowacki, W. *Thermoelasticity*; Pergamon Press: New York, NY, USA, 1962.
2. Sih, G.C.; Michaopoloulos, J.; Chou, S.C. *Hygrothermoelasticity*; Martinus Niijhoof Publishing: Leiden, The Netherlands, 1986.
3. Sih, G.C. *Mechanics of Fracture Initiation and Propagation*; Kluwer Academic Publishers: Boston, MA, USA, 1991.
4. Sih, G.C. Thermomechanics of solids: Nonequilibrium and irreversibility. *Theor. Appl. Fract. Mech.* **1988**, *9*, 175–198. [CrossRef]
5. Yang, J.; Jin, X.Y.; Jin, N.G. A penny-shaped crack in an infinite linear transversely isotropic medium subjected to uniform anti-symmetric heat flux: Closed-form solution. *Eur. J. Mech.-A Solids* **2014**, *47*, 254–270. [CrossRef]
6. Zhong, X.C.; Long, X.Y.; Zhang, L.H. An extended thermal-medium crack model. *Appl. Math. Model.* **2017**, *56*, 202–216. [CrossRef]
7. Tsai, Y.M. Orthotropic thermoelastic problem of uniform heat flow disturbed by a central crack. *J. Compos. Mater.* **1984**, *18*, 122–131. [CrossRef]
8. Ju, S.H.; Rowlands, R.E. Mixed-mode thermoelastic fracture analysis of orthotropic composites. *Int. J. Fract.* **2003**, *120*, 601–621. [CrossRef]
9. Chen, B.X.; Zhang, X.Z. Thermo-elasticity problem of an orthotropic plate with two collinear cracks. *Int. J. Fract.* **1988**, *38*, 161–192.

10. Noda, N. Transient thermal stress problem in an orthotropic thin plate with a Griffith crack. *Ing.-Arch.* **1987**, *57*, 175–181. [CrossRef]
11. Rizk, A.A. Orthotropic semi-infinite medium with a crack under thermal shock. *Theor. Appl. Fract. Mech.* **2006**, *46*, 217–231. [CrossRef]
12. Kim, J.; Paulino, G. Mixed-mode fracture of orthotropic functionally graded materials using finite elements and the modified crack closure method. *Eng. Fract. Mech.* **2002**, *69*, 1557–1586. [CrossRef]
13. Brock, L.M. Reflection and diffraction of plane temperature-step waves in orthotropic thermoelastic solids. *J. Therm. Stress.* **2010**, *33*, 879–904. [CrossRef]
14. Dag, S. Thermal fracture analysis of orthotropic functionally graded materials using an equivalent domain integral approach. *Eng. Fract. Mech.* **2006**, *73*, 2802–2828. [CrossRef]
15. Wu, B.; Zhu, J.G.; Peng, D.; Jones, R.; Gao, S.H.; Lu, Y.Y. Thermoelastic analysis for two collinear cracks in an orthotropic solid disturbed by anti-symmetrical linear heat flow. *Math. Probl. Eng.* **2017**, *2017*, 5093404. [CrossRef]
16. Ootao, Y.; Tanigawa, Y. Transient thermal stresses of orthotropic functionally graded thick strip due to nonuniform heat supply. *Struct. Eng. Mech.* **2005**, *20*, 559–573. [CrossRef]
17. Wu, C.H. Plane anisotropic thermoelasticity. *J. Appl. Mech.* **1984**, *51*, 724–726. [CrossRef]
18. Liu, L.; Kardomateas, G.A. A dislocation approach for the thermal stress intensity factors of a crack in an anisotropic medium under uniform heat flow. *Compos. Part A* **2006**, *37*, 989–996. [CrossRef]
19. Xue, Z.; Evans, A.G.; Hutchinson, J.W. Delamination susceptibility of coatings under high thermal flux. *J. Appl. Mech.* **2009**, *76*, 728–731. [CrossRef]
20. Zhou, Y.T.; Li, X.; Yu, D.H. Partially impermeable interface crack between a graded orthotropic coating and a homogeneous orthotropic substrate under heat flux supply. *Int. J. Solids Struct.* **2010**, *47*, 768–778. [CrossRef]
21. Nowinski, J.L. *Theory of Thermoelasticity with Applications*; Sijthoff and Noordhoff: Dordrecht, The Netherlands, 1978.
22. Barber, J.R. Imperfectly conducting penny-shaped crack in an elastic solid. *J. Therm. Stress* **1980**, *3*, 77–83. [CrossRef]
23. Kuo, A.Y. Effects of crack surface heat conductance on stress intensity factors. *J. Appl. Mech.* **1990**, *57*, 354–358. [CrossRef]
24. Wu, B.; Peng, D.; Jones, R. The analysis of cracking under a combined quadratic thermal flux and a quadratic mechanical loading. *Appl. Math. Model.* **2019**, *68*, 182–197. [CrossRef]
25. Gradshteyn, I.S.; Ryzhik, I.M. *Table of Integrals, Series, and Products*; Elsevier Academic Press: Berkeley, CA, USA, 2007.
26. Zhong, X.C.; Wu, B.; Zhang, K.S. Thermally conducting collinear cracks engulfed by thermo-mechanical field in a material with orthotropy. *Theor. Appl. Fract. Mech.* **2013**, *65*, 61–68. [CrossRef]
27. Gdoutos, E.E. Solid Mechanics and Its Applications. In *Fracture Mechanics: An Introduction*, 3rd ed.; Springer Nature: Cham, Switzerland, 2020; ISBN 978-3-030-35097-0.
28. Sih, G.C.; Paris, P.; Irwin, G.R. On cracks in rectilinearly anisotropic bodies. *Int. J. Fract.* **1965**, *1*, 189–203. [CrossRef]
29. Itou, S. Thermal stress intensity factors of an infinite orthotropic layer with a crack. *Int. J. Fract.* **2000**, *103*, 279–291. [CrossRef]
30. Peng, D.; Jones, R.; Pitt, S. A hybrid formulation for 3D fracture analysis. *Eng. Fract. Mech.* **2002**, *69*, 45–67. [CrossRef]
31. Jones, R.; Peng, D.; Pitt, S.; Wallbrink, C. Weight Functions, CTOD, and Related Solutions for Cracks at Notches. *Eng. Fail. Anal.* **2004**, *11*, 79–114. [CrossRef]
32. Belardi, V.G.; Fanelli, P.; Vivio, F. Structural analysis of transversally loaded quasi-isotropic rectilinear orthotropic composite circular plates with Galerkin method. *Procedia Struct. Integr.* **2018**, *8*, 368–378. [CrossRef]
33. Belardi, V.G.; Fanelli, P.; Vivio, F. Bending analysis with Galerkin method of rectilinear orthotropic composite circular plates subject to transversal load. *Compos. Part B Eng.* **2018**, *140*, 250–259. [CrossRef]
34. Kabir, H.; Aghdam, M.M. A robust Bézier based solution for nonlinear vibration and post-buckling of random checkerboard graphene nano-platelets reinforced composite beams. *Compos. Struct.* **2019**, *212*, 184–198. [CrossRef]
35. Kabir, H.; Aghdam, M.M. A generalized 2D Bézier-based solution for stress analysis of notched epoxy resin plates reinforced with graphene nanoplatelets. *Thin-Walled Struct.* **2021**, *169*, 108484. [CrossRef]